MITSUBISHI ELECTRIC RESEARCH LABORATORIES
http://www.merl.com

A Dual-Mode Bias Circuit Enabled GaN Doherty Amplifier Operating in 0.85-2.05GHz and 2.4-4.2GHz

Komatsuszaki, Yuji; Ma, Rui; Sakata, Shuichi; Nakatani, Keigo; Shinjo, Shintaro

TR2020-080 June 24, 2020

Abstract

We report an ultra-wideband and high efficiency sub-6GHz power amplifier, which is based on multi-band Doherty load modulation. Key novelty is that a dual-mode bias circuit which operate as frequency-dependent compensating circuit at a half of center frequency 0.5f0 mode, and DC-block and RF-choke at a center frequency f0 mode. The amplifier using 0.15-um GaN HEMT FETs achieved drain efficiency of 41.4-58.2% over 0.85-2.05GHz with 0.5f0 mode, and 43.5-62.1% over 2.4-4.2GHz with f0 mode at 6dB power back-off. This, to the best of authors' knowledge, is the widest coverage of frequency reported so far for a multi-band Doherty amplifier at these carrier frequency range. It is a very promising PA technology for sub 6GHz base station, enabling reduction of the total cost of ownership (TCO) for operators.

IEEE International Microwave Symposium (IMS)

A Dual-Mode Bias Circuit Enabled GaN Doherty Amplifier Operating in 0.85-2.05GHz and 2.4-4.2GHz

Yuji Komatsuzaki[#1], Rui Ma[*], Shuichi Sakata[#], Keigo Nakatani[#], Shintaro Shinjo[#]
[#] Mitsubishi Electric Corporation, Information Technology R&D Center, Japan
[*] Mitsubishi Electric Research Laboratories, USA
[1] Komatsuzaki.Yuji@bx.MitsubishiElectric.co.jp

***Abstract*— We report an ultra-wideband and high efficiency sub-6GHz power amplifier, which is based on multi-band Doherty load modulation. Key novelty is that a dual-mode bias circuit which operate as frequency-dependent compensating circuit at a half of center frequency $0.5f_0$ mode, and DC-block and RF-choke at a center frequency f_0 mode. The amplifier using 0.15-μm GaN HEMT FETs achieved drain efficiency of 41.4-58.2% over 0.85-2.05GHz with $0.5f_0$ mode, and 43.5-62.1% over 2.4-4.2GHz with f_0 mode at 6dB power back-off. This, to the best of authors' knowledge, is the widest coverage of frequency reported so far for a multi-band Doherty amplifier at these carrier frequency range. It is a very promising PA technology for sub-6GHz base station, enabling reduction of the total cost of ownership (TCO) for operators.**

***Keywords*— GaN, power amplifier, Doherty amplifier, bias circuit, load modulation.**

I. Introduction

Recently, advanced wireless communication systems apply high peak-to-average power ratio (PAPR) signals to cope with crowded spectrum and higher speed data demands. RF power amplifiers (PA) for base stations require high efficiency at a large back-off power level. In particular, an RF amplifier covering frequency up to 6GHz becomes increasingly important for next generation mobile communication systems, such as sub-6GHz 5G to achieve high capacity communication, while maintaining backward compatibility for 3G-4G system. At present, Doherty Power Amplifier (DPA) is widely deployed in base stations. However, DPA is fundamentally limited to narrow frequency range due to the frequency dependent 90˚ transmission line for load modulation. Hence, to expand bandwidth with high efficiency of PA, circuit technologies to widen the bandwidth of DPA [1] and various non-Doherty configuration have been studied [2]-[4]. On the other hand, to enhance the performance of ultra-wideband PAs, low-loss and wide-band output bias circuit is necessary.

In this paper, we report a multi-band DPA with 0.85-2.05GHz and 2.4-4.2GHz modes. It is enabled with a dual-mode bias circuit. A novel drain bias circuit to achieve high efficiency at back-off over both frequency modes is designed and demonstrated. Our DPA employs output circuit which operates as multi-mode load modulation combiner included at least 2-types of Doherty modes [2], [4]-[5] over frequency. The input circuit includes wideband power divider and phase shifter to equalize electric length of a main and an auxiliary amplifier chain. Then, a 0.85-2.05GHz half of center frequency mode and a 2.4-4.2GHz center frequency mode are exchanged via changing the role of the main and the auxiliary amplifier by switching gate bias conditions. In the description, the center frequency is denoted as f_0. Notably, the dual-mode bias circuit operates as frequency-dependent compensating circuit at $0.5f_0$ mode, and DC-block and RF-choke at f_0 mode. The multi-band DPA achieves drain efficiency of 41.4-58.2% over 0.85-2.05GHz $0.5f_0$ mode and 43.5-62.1% over 2.4-4.2GHz f_0 mode at 6dB back-off level. We successfully demonstrated the new concept of multi-band DPA with dual-mode bias circuit in the experiment.

II. Multi-Band Doherty Amplifier with Multi-Mode Bias Circuit

A. Circuit Configuration

The schematic of circuit diagram of multi-band DPA with dual-mode bias circuit is shown in Fig. 1. The circuit employs two GaN FETs. The equivalent transmission line is connected to each FET at the equivalent current source plane of the device. Device parasitic capacitance C_{ds} is absorbed into the equivalent transmission line. An additional transmission line with electrical length of 90˚ at the center frequency is further connected to one side of the FETs. Characteristic impedance of the combiner based on above transmission lines is chosen to be the optimum load resistance of FET, R_{opt}. Dual-mode bias circuit and output matching network (OMN) are connected at the output of the combiner. In the input side, input matching networks (IMN) including stabilization circuit, a divider and 90˚ transmission line are connected.

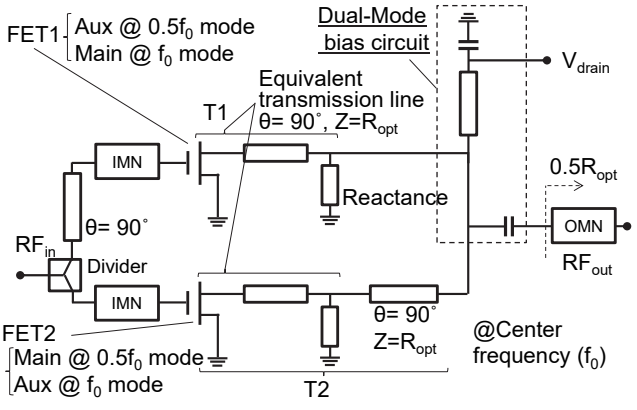

Fig. 1. Schematic of the circuit diagram of multi-band DPA with $0.5f_0$ and f_0 with dual-mode bias circuit.

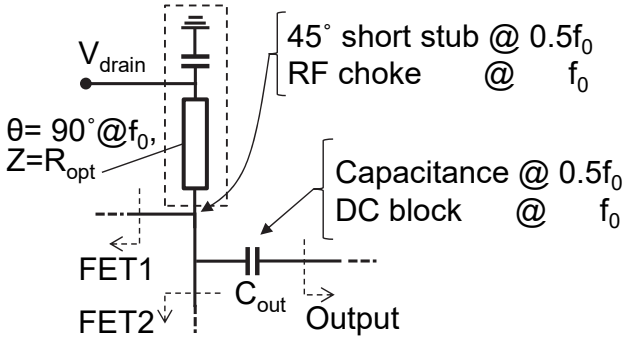

Fig. 2. Schematic of the dual-mode bias circuit.

The amplifier has two operation mode described as $0.5f_0$ mode and f_0 mode, respectively. At f_0 mode, 90˚ equivalent transmission line for load modulation is connected at output of FET1. Then, the gate bias voltages of FET1 and FET2 are biased above and below the threshold point of FETs. In this case, FET1 and FET2 operate as a main and an auxiliary amplifier, respectively. On the other hand, at $0.5f_0$ mode, 90˚ equivalent transmission line is connected at output of FET2, the biases of FET1 and FET2 are exchanged. Then, FET1 and FET2 operate as an auxiliary and a main amplifier, respectively.

The concept of dual-mode bias circuit is shown in Fig. 2. The key idea is to apply it as both frequency-dependent compensating circuit to widen band-width at $0.5f_0$ mode, and as DC-block and RF-choke at f_0 mode.

B. Circuit Operation with RF Frequency

In this section, the difference of load modulation and the operation of dual-mode bias circuit for each $0.5f_0$ and f_0 mode are explained in details.

At $0.5f_0$ mode, the FET1 operates as an auxiliary amplifier, and FET2 operates as a main amplifier. At the back-off level, the FET1 is turned off, so the output terminal of FET1 is open as shown in Fig. 3. Normalized impedance Z_0 of Smith chart in Fig. 3 is R_{opt}. At a frequency of $0.5f_0$, 45˚ open (T1) and 45˚ short (bias) stubs are in parallel, therefore they are cancelling each other, and thus do not affect the load modulation of 90˚ transmission line at FET2. On the other hand, the load modulation of the transmission line (shorter than 90˚ below $0.5f_0$ and longer than 90˚ above $0.5f_0$), is compensated with the open and short stubs, since it behaves as inductive circuit below $0.5f_0$ and capacitive circuit above $0.5f_0$, respectively. At the saturated power level, T1 works as transmission line as shown in Fig. 4. Normalized impedance Z_0 of Smith chart in Fig. 4 is $0.5R_{opt}$. Therefore, only the 45˚ short (bias) stub remains and the output capacitor C_{out} compensates impedance mismatching caused by the stub. It has been noted that the C_{out} value is properly chosen not to affect load modulation at back-off level. Fig. 5a shows simulated frequency response of reflection with $0.5f_0$ mode at output terminal of main FET current source at back off level, and it demonstrates that bias circuit enhances the bandwidth of load modulation, even with C_{out}. Fig. 5b shows reflection at output terminal of PA at saturated level, and it demonstrates that C_{out} can reduce the reflection.

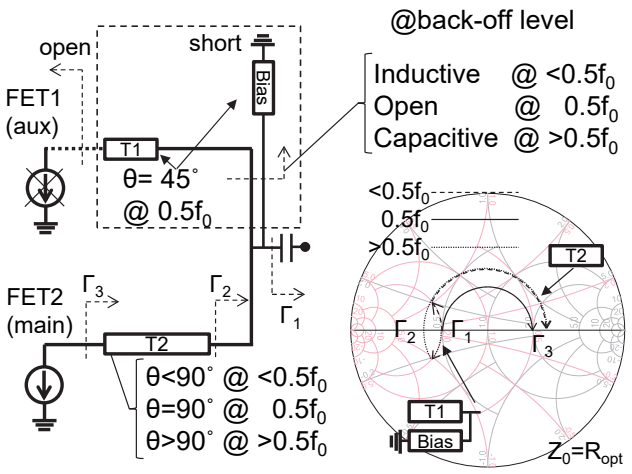

Fig. 3. Circuit configuration and impedance transformation trace of the DPA with $0.5f_0$ mode at back-off level.

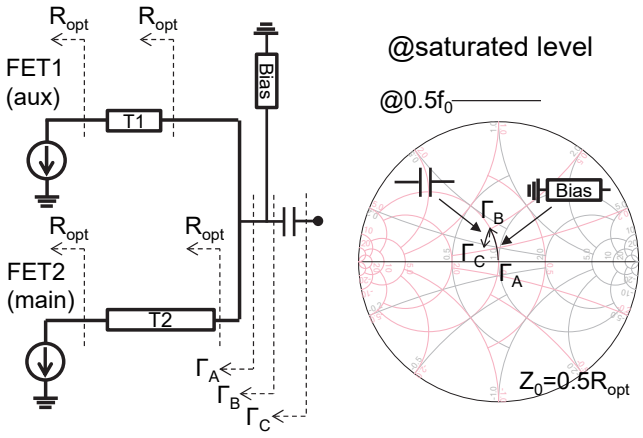

Fig. 4. Circuit configuration and impedance transformation trace of the DPA with $0.5f_0$ mode at saturated level.

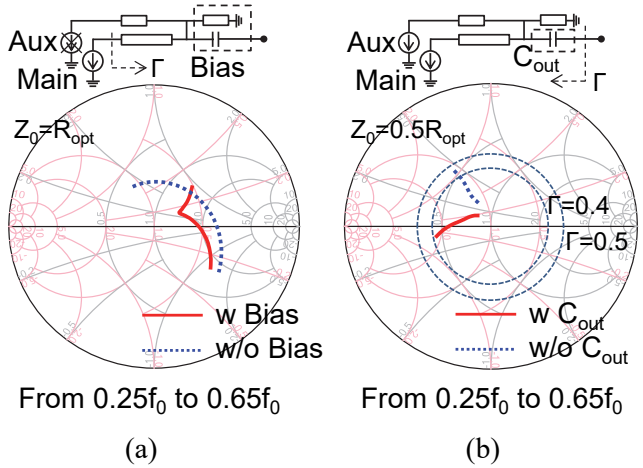

Fig. 5. Simulated frequency response of reflection with $0.5f_0$ mode: (a) output terminal of main FET current source at back-off level; (b) output terminal of DPA at saturated level.

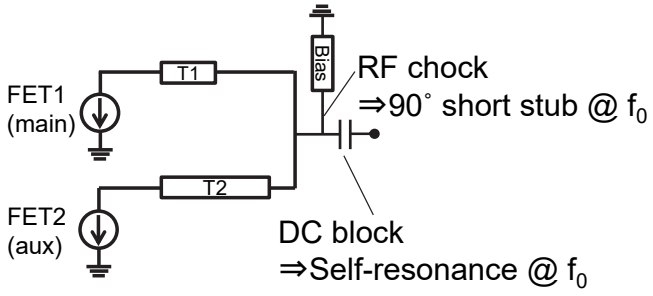

Fig. 6. Circuit configuration of the DPA with f_0 mode.

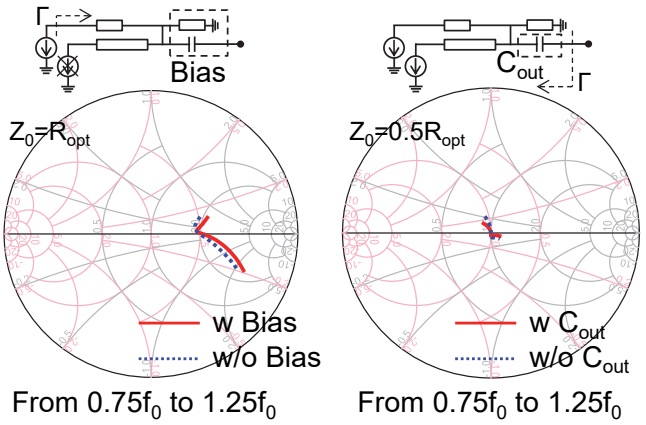

Fig. 7. Simulated frequency response of reflection with f_0 mode: (a) output terminal of main FET current source at back-off level; (b) output terminal of DPA at saturated level.

At f_0 mode, FET1 operates as a main amplifier, and FET2 operates as an auxiliary amplifier. At a frequency of f_0, the bias circuit consists of 90˚ short stub and C_{out} which is self-resonated as shown in Fig. 6. Thus, the bias circuit operates as DC-block and RF-choke. Fig. 7 shows the simulated frequency response of reflection with f_0 mode. It demonstrates that the bias circuit does not affect matching for both back-off and saturated levels.

III. Measurement Result

Fig. 8 shows the photo of the assembled GaN multi-band DPA with dual-mode bias circuit. Upper one is FET1, and lower one is FET2. In this work, OMN to 50Ω load in Fig. 1 is not needed, because transistor R_{opt} is synthesized to be 100Ω.

Fig. 9 and Fig. 10 show the measured drain efficiency and gain characteristics with power sweep at different frequency. The DPA operates as $0.5f_0$ mode in Fig. 9 and f_0 mode in Fig. 10, respectively. At $0.5f_0$ mode, FET1 is biased as an auxiliary amplifier and FET2 is biased as a main amplifier. At f_0 mode, operation of FET1 and FET2 is exchanged against $0.5f_0$ mode, FET1 is biased as a main amplifier and FET2 is biased as an auxiliary amplifier. The drain voltage is 28V. Both $0.5f_0$ and f_0 modes operation clearly demonstrate one can obtain efficiency peak of Doherty load modulation at around 6dB back-off level.

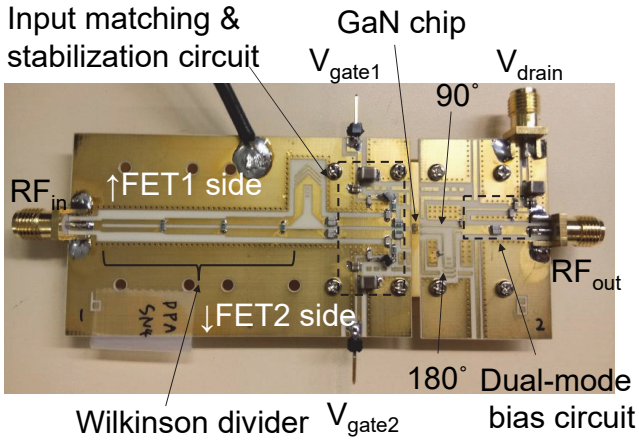

Fig. 8. Photo of the assembled 0.15μm-GaN HEMT multi-band DPA with $0.5f_0$ and f_0 with dual-mode bias circuit.

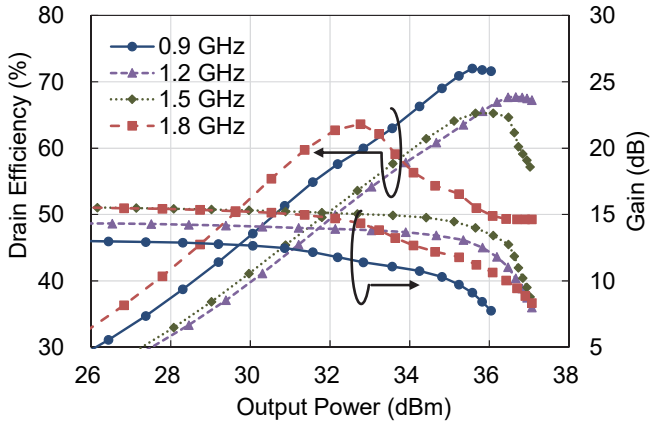

Fig. 9. Measured drain efficiency and gain with power sweep at different frequency of $0.5f_0$ mode.

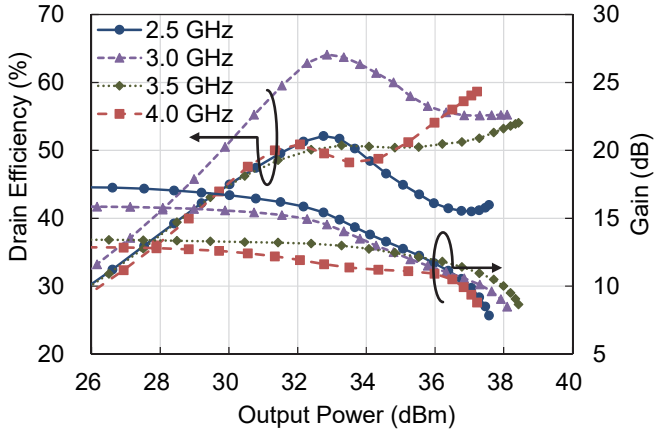

Fig. 10. Measured drain efficiency and gain with power sweep at different frequency of f_0 mode.

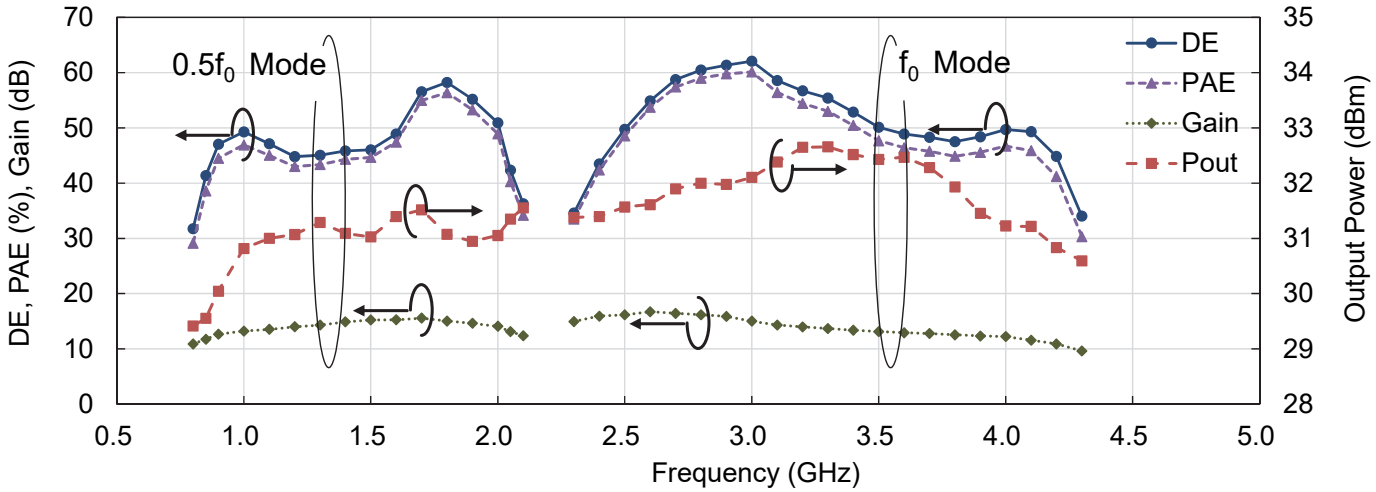

Fig. 11. Measured frequency dependences of drain efficiency (DE), power added efficiency (PAE), gain, and output power at 6dB power back-off level.

Table 1. Comparison of sub-6GHz high efficiency wideband amplifiers.

Ref.	Year	Freq. (GHz)	Fractional BW(%)	Efficiency (%)	Pout (dBm)	Configutration	backoff
[1]	2012	3.0-3.6	18	38-56	37-38	Doherty	6dB(CW)
[2]	2013	1.0-3.0	100	48-68	37.1-38.9	Doherty/Outphasing	6dB(CW)
[3]	2017	0.9-2.15	82	32-36	30.0-30.7	Envelope tracking	6.5dB(Mod.)
[6]	2016	2.05-2.3	11	48-52	41.3	Multi-band Doherty	6dB(CW)
		3.2-3.6	12	42-51	41		
[4]	2019	1.4-4.8	110	45-62	29.9-32.8	Doherty/Outphasing	6dB(CW)
[5]	2019	2.2-2.7	20	40-52	33-35	Multi-band Doherty	6dB(CW)
		2.8-4.1	38	42-50	34-35		
		4.2-4.8	13	36-43	33-35		
Here	2019	0.85-2.05	83	41-58	29.6-31.5	Multi-band Doherty	6dB(CW)
		2.4-4.2	55	44-62	30.8-32.7		

Fig. 11 shows measured ultra-wide bandwidth of the designed amplifier. 41.4-58.2% of drain efficiency is achieved with $0.5f_0$ mode across the measured frequency range 0.85-2.05GHz, and 43.5-62.1% of drain efficiency is achieved with f_0 mode across the measured frequency range 2.4-4.2GHz at 6dB power back-off level. Output power at 6dB back-off is approximately 31.5dBm. Fractional bandwidth of 83% and 55% is achieved with $0.5f_0$ mode and f_0 mode, respectively. This, to the best of the authors' knowledge, is the one of the widest coverage of frequency reported so far for a multi-band DPA at these carrier frequency range.

Table 1 shows the state-of-the-art performance of sub-6GHz wideband amplifiers with high efficiency. Compared with other reported amplifiers, this new multi-band DPA with dual-mode bias circuit reported has the one of the widest bandwidth with drain efficiency over 41%.

IV. Conclusion

By exploring a novel Doherty output combiner topology included the bias circuit and leveraging its dual-mode operation, the demonstrated GaN DPA maintains high average efficiency over the wide fractional bandwidth, relying on frequency-dependent compensated load modulation mechanism. The use of the wideband efficient DPA assisted by cutting-edge GaN HEMT technology can reduce the complexity and energy consumption of radio, which further helps reducing TCO of next generation wireless communication base stations.

References

[1] J. M. Rubio, J. Fang, V. Camarchia, R. Quaglia, M. Pirola, and G. Ghione, "3–3.6-GHz Wideband GaN Doherty Power Amplifier Exploiting Output Compensation Stages," *IEEE Trans. Microw. Theory Techn.*, vol. 60, no. 8, pp. 2543-2548, August 2012.

[2] C. M. Andersson, D. Gustafsson, J. C. Cahuana, R. Hellberg, and C. Fager, "A 1–3-GHz Digitally Controlled Dual-RF Input Power-Amplifier Design Based on a Doherty-Outphasing Continuum Analysis," *IEEE Trans. Microw. Theory Techn.*, vol. 61, no. 10, pp. 3743-3752, October 2013.

[3] S. Sakata, S. Lanfranco, T. Kolmonen, O. Piirainen, T. Fujiwara, S. Shinjo, and P. Asbeck, "An 80MHz Modulation Bandwidth High Efficiency Multi-band Envelope-Tracking Power Amplifier Using GaN Single-Phase Buck-Converter," *2017 IEEE MTT-S Int. Microw. Symp.,* Honolulu, HI.

[4] Y. Komatsuzaki, R. Ma, M. Benosman, Y. Nagai, S. Sakata, K. Nakatani, and S. Shinjo, "A Novel 1.4-4.8 GHz Ultra-Wideband, over 45% High Efficiency Digitally Assisted Frequency-Periodic Load Modulated Amplifier," *2019 IEEE MTT-S Int. Microw. Symp.,* Boston, MA.

[5] M. Li, J. Pang, Y. Li, and A. Zhu, "Ultra-Wideband Dual-Mode Doherty Power Amplifier Using Reciprocal Gate Bias for 5G Applications," *IEEE Trans. Microw. Theory Techn.*, vol. 67, no. 10, pp. 4246-4259, October 2019.

[6] M. Liu, H. Golestaneh, and S. Boumaiza, "A concurrent 2.15/3.4 GHz dual-band Doherty power amplifier with extended fractional bandwidth," *2016 IEEE MTT-S Int. Microw. Symp.,* San Francisco, CA.